Optical force calculations in arbitrary beams by use of the vector addition theorem

Olivier Moine and Brian Stout

Institut Fresnel, Unité Mixte de Recherche 6133, Université Aix-Marseille I, Case 161 Faculté des Sciences et Techniques, Centre de Saint Jérome, 13397 Marseille Cedex 20, France.

Received September 24, 2004; revised manuscript received February 11, 2005; accepted February 15, 2005

We derive and apply formulas that employ the vector-wave addition theorem and rotation matrices for quantitative calculations of both radial and axial optical forces exerted on particles trapped in arbitrarily shaped tweezer beams. For the tightly focused beams encountered in optical tweezers, we shall highlight the importance of formulating the optical forces and beam symmetries in terms of the irradiance and total beam power. A major interest of the addition theorem treatment of optical forces is that it opens up the possibility of modeling a wide variety of beam shapes while automatically ensuring that the beams satisfy the Maxwell equations. In some of the first numerical applications of our method, we shall illustrate that resonance effects play an important role in the axial trapping position of particles comparable in size with the wavelength of the trapping beam.

OCIS codes: 140.7010, 140.3300, 120.5820, 290.4020.

1. INTRODUCTION

Optical tweezers and traps have opened up a new domain of laser applications in that they allow the mechanical manipulation of particles via light-induced forces.[1] The essential aspect of optical tweezers is to create large gradients in the field intensity that induce optical forces that attract dielectric particles toward regions of high intensity. Outside their demonstrated usefulness to trap, displace, and rotate particles, a major interest of optical tweezers is the measurement of molecular scale forces that, like typical optical forces, are frequently in the 1–100 (pN) range.[2–6] A reliable theory of optical forces is therefore useful in this regard.

Particles commonly trapped in optical tweezers experiments of characteristic size D are frequently too large to be reliably treated in a simple dipole model,[7] $D \ll \lambda$, and not large enough to be reliably treated via a geometrical optics approach,[8] $D \gg \lambda$. The weak dielectric contrast of many optically trapped particles has motivated the use of Born-type approximations[9] for particles in the intermediate or resonant size regime, $D \sim \lambda$, but this method is reliable only to the extent in which the particle only weakly modifies the incident beam, and the precise domain of validity of this approximation is not known. Consequently, optical force experiments are frequently carried out by one's experimentally measuring the forces on spherical particles and then attaching these calibrated optical handles to the molecules, membranes, or cells under study.[10]

Optical force calculations based on transition matrices[11,12] (or a Lorentz–Mie-type theory for spheres[13]) are an obvious choice for rigorous numerical calculations of the optical force. We demonstrate in this paper that quantitative calculations of the force along an arbitrary direction can be performed by invoking the translation-addition matrices familiar from analytic multiple-scattering calculations.[11] Another important aspect of quantitative calculations is the necessity to accurately model realistic optical tweezer beams. Space does not permit a detailed discussion of the various possible beam shapes in this paper, but we shall discuss the partial-wave decomposition of focused laser beams and the importance of irradiance when evaluating beam symmetries and optical forces.

Although our transition-matrix formulas can be applied to arbitrary scatterers, in the interest of simplicity, we shall restrict our attention to the optical forces on dielectric spheres suspended in liquid dielectrics. For the purpose of theoretical comparisons, we simply study here some simple models based on Davis-type corrections to Gaussian-type focused beams.[14,15] Although these models are rather poor approximations to realistic tweezer beams, they have the advantage of having rather simple partial-wave expansions. These models suffice, nevertheless, to illustrate the necessity of proper beam normalization and the importance of an irradiance formulation of the beam symmetries.

The principal goal of this paper is to present our technique of calculation and to illustrate its ability to perform quantitative calculation of optical forces on resonant dielectric particles $D \gtrsim \lambda$. Our techniques can be adopted to the study of non-Gaussian beams (doughnut beams, top-hat beams, Bessel beams, etc.) and can be used to systematically test the domain of application of the various approximate theories. These topics, however, shall be treated in subsequent publications.

We use SI units throughout this paper. In view of the scale-invariant nature of the electromagnetic equations,

0740-3224/05/081620-12/$15.00

we shall formulate our results in terms of dimensionless parameters wherever possible. Nevertheless, numerical applications will be formulated for the commonly employed infrared optical tweezer beams with a vacuum wavelength of $\lambda_0 = 1.064$ (μm). Water is assumed for the background liquid dielectric media, $n_b \simeq 1.32$, and the trapped particles will be either silica $n_s \simeq 1.46$ or latex $n_s \simeq 1.59$.

We have broken this paper up into three largely independent sections. Section 2 is dedicated to introducing the partial-wave developments of the electromagnetic fields and a discussion of beam symmetries and normalization. Section 3 presents our expressions for the optical forces derived from the Maxwell constraint tensor. The translation-addition theorem of scattering theory permits the calculation of the forces at different positions, whereas the angular-momentum rotation formulas permit the calculation of the forces in different directions. Indicative calculations are presented in this section for both radial and axial forces. We also present some preliminary results demonstrating the importance of resonance effects on the trapping position of large particles.

2. ELECTROMAGNETIC PARTIAL WAVES

We adopt a time-harmonic incident field with an $\exp(-i\omega t)$ time dependence and assume that trapped particles are suspended in a homogeneous absorption-free liquid dielectric medium. The time-harmonic Maxwell equations then require that the electric field in a homogenous medium satisfies the following second-order differential equation:

$$\nabla \times \nabla \times \mathbf{E}(\mathbf{r}) - k^2 \mathbf{E}(\mathbf{r}) = 0, \tag{1}$$

with $k = \sqrt{\varepsilon_b \mu_0}\sqrt{\epsilon_0 \mu_0}\omega = n_b \omega / c$, where (ϵ_0, μ_0) are the permittivity and the permeability of the vacuum and (ε_b, μ_b) are the relative permittivity and the permeability of the background dielectric medium. The electromagnetic partial waves or vector spherical wave functions (VSWFs) are a set of spherical waves centered on a given origin and form a complete basis set of solutions to Eq. (1).

The set of outgoing (or irregular[11]) VSWFs is traditionally denoted by $\mathbf{M}_{n,m}$, $\mathbf{N}_{n,m}$ and satisfies Eq. (1) with outgoing boundary conditions:

$$\begin{aligned}
\mathbf{M}_{nm}(k\mathbf{r}) &\equiv h_n(kr)\mathbf{X}_{nm}(\theta,\phi),\\
\mathbf{N}_{nm}(k\mathbf{r}) &\equiv \frac{1}{kr}\{\sqrt{n(n+1)}h_n(kr)\mathbf{Y}_{nm}(\theta,\phi)\\
&\quad + [krh_n(kr)]'\mathbf{Z}_{nm}(\theta,\phi)\},
\end{aligned} \tag{2}$$

where h_n are the spherical Hankel functions of the first kind and $[krh_n(kr)]'$ is the derivative of $krh_n(kr)$ with respect to kr. We use a normalized version of the **M** and **N** functions,[11] which can be conveniently expressed in terms of the normalized vector spherical harmonics (VSHs) **X**, **Y**, and **Z**[16]:

$$\begin{aligned}
\mathbf{X}_{nm}(\theta,\phi) &\equiv \mathbf{Z}_{nm}(\theta,\phi)\times\hat{\mathbf{r}} = \gamma_{nm}\mathbf{C}_{nm}(\theta,\phi),\\
\mathbf{Y}_{nm}(\theta,\phi) &\equiv \hat{\mathbf{r}}Y_{nm}(\theta,\phi) \equiv \gamma_{nm}\sqrt{n(n+1)}\mathbf{P}_{nm}(\theta,\phi),\\
\mathbf{Z}_{nm}(\theta,\phi) &\equiv \frac{r\nabla Y_{nm}(\theta,\phi)}{\sqrt{n(n+1)}} = \hat{\mathbf{r}}\times\mathbf{X}_{nm}(\theta,\phi)\\
&= \gamma_{nm}\mathbf{B}_{nm}(\theta,\phi),
\end{aligned} \tag{3}$$

where $Y_{nm}(\theta,\phi)$ are the normalized scalar spherical harmonics and **C**, **P**, **B** are the VSHs used by Tsang *et al.*[11] (see also Appendix A). Nondivergent (i.e., incident) fields should be developed on the basis of regular partial waves, $\mathcal{R}g\{[\mathbf{M}_{n,m}]\}$, $\mathcal{R}g\{[\mathbf{N}_{n,m}]\}$,[11] which are obtained by one's replacing the spherical Hankel functions, h_n, in Eqs. (2) with spherical Bessel functions j_n.

A. Partial-Wave Developments of the Incident Field

The above results permit the development of an arbitrary incident electric field, $\mathbf{E}_i(\mathbf{r})$, on the basis of the regular VSWFs:

$$\begin{aligned}
\mathbf{E}_i(\mathbf{r}) &= A\sum_{n,m}\mathcal{R}g\{[\mathbf{M}_{n,m}(k\mathbf{r})]\}a^{\mathrm{M}}_{n,m} + \mathcal{R}g\{[\mathbf{N}_{n,m}(k\mathbf{r})]\}a^{\mathrm{N}}_{n,m}\\
&\equiv A\mathcal{R}g\{[\mathbf{M}(k\mathbf{r}),\mathbf{N}(k\mathbf{r})]\}a\\
&\equiv A\mathcal{R}g\{\boldsymbol{\Psi}^t(k\mathbf{r})\}a,
\end{aligned} \tag{4}$$

where A is an overall field amplitude coefficient with the dimensions of an electric field and $a^{\mathrm{M}}_{n,m}$, $a^{\mathrm{N}}_{n,m}$ are dimensionless partial-wave expansion coefficients. The second and third lines of Eq. (4) introduce a compact vector notation that allows the suppression of the bothersome summation over index labels, n, m.[11,12] In the compact notation, a is a shorthand symbol representing an infinite column vector composed of the $a^{\mathrm{M}}_{n,m}$, $a^{\mathrm{N}}_{n,m}$ coefficients, and $\boldsymbol{\Psi}^t$ (the t indicating the transpose) represents an infinite row vector composed of the VSWFs:

$$\boldsymbol{\Psi}(k\mathbf{r}) = [\mathbf{M}_{1,1}(k\mathbf{r}),\mathbf{M}_{1,0}(k\mathbf{r}),\mathbf{M}_{1,-1}(k\mathbf{r}),\ldots,\mathbf{N}_{1,1}(k\mathbf{r}),\mathbf{N}_{1,0}(k\mathbf{r}),\mathbf{N}_{1,-1}(k\mathbf{r}),\ldots]. \tag{5}$$

One can find the incident magnetic field corresponding to a given incident electric field by invoking Faraday's law,

$$\mathbf{H}_{\mathrm{i}}(\mathbf{r}) = \frac{1}{i\omega\mu_b\mu_0}\nabla\times\mathbf{E}_{\mathrm{i}}(\mathbf{r}) = \frac{A}{i\omega\mu_b\mu_0}\mathcal{R}g\{\nabla\times\boldsymbol{\Psi}^t(k\mathbf{r})\}a$$
$$= A\left(\frac{\varepsilon_b\epsilon_0}{\mu_b\mu_0}\right)^{1/2}\mathcal{R}g\{[\mathbf{N}(k\mathbf{r}),\mathbf{M}(k\mathbf{r})]\}a, \quad (6)$$

and the convenient rotational properties of the VSWFs, $\nabla\times\mathbf{M}=k\mathbf{N}$ and $\nabla\times\mathbf{N}=k\mathbf{M}$.

The most common theoretical choice for incident fields in electromagnetic theory is that of polarized homogenous incident plane waves of the form $\mathbf{E}_{\mathrm{i}}^{\mathrm{p.w.}}=A\exp(i\mathbf{k}_{\mathrm{i}}\cdot\mathbf{r})\hat{\mathbf{e}}_{\mathrm{i}}$, where $\hat{\mathbf{e}}_{\mathrm{i}}$ is a (possibly complex) polarization vector with unit norm $|\hat{\mathbf{e}}_{\mathrm{i}}|=1$. For this choice, the incident-field coefficients can be determined analytically and can be conveniently expressed in terms of the VSHs[16]:

$$[p]_{nm}^{\mathrm{M}} \equiv 4\pi\mathcal{X}_{nm}(\hat{\mathbf{k}}_{\mathrm{i}})\cdot\hat{\mathbf{e}}_{\mathrm{i}} \equiv 4\pi i^n\mathbf{X}_{nm}^{*}(\hat{\mathbf{k}}_{\mathrm{i}})\cdot\hat{\mathbf{e}}_{\mathrm{i}},$$

$$[p]_{nm}^{\mathrm{N}} = 4\pi\mathcal{Z}_{nm}(\hat{\mathbf{k}}_{\mathrm{i}})\cdot\hat{\mathbf{e}}_{\mathrm{i}} \equiv 4\pi i^{n-1}\mathbf{Z}_{nm}^{*}(\hat{\mathbf{k}}_{\mathrm{i}})\cdot\hat{\mathbf{e}}_{\mathrm{i}}, \quad (7)$$

where we replace the arbitrary incident-field coefficient vector a with the symbol p as a reminder that the $[p]_{nm}^{\mathrm{M,N}}$ are the coefficients of an incident plane wave. It proves convenient to define the phase-modified VSH, $\mathcal{X}_{nm}$ and $\mathcal{Z}_{nm}$, in Eqs. (7) because these quantities appear repeatedly in far-field calculations.

For inhomogeneous beams such as those used in optical tweezers, the normalization of the field amplitude coefficient A in Eq. (4) can easily become a point of confusion and erroneous results. For the common optical tweezer beams formed from a lowest-order T_{00}-type laser mode, we choose to normalize the field amplitude at the maximal symmetry point of the beam (i.e., the center of the Rayleigh region—typically being the point of maximal field amplitude). When this maximal symmetry point is taken to be the system origin, O, the connection with experimental irradiance is facilitated if we define A such that

$$A^2 \equiv 2|\mathbf{S}_{\mathrm{i}}(\mathbf{0})|\left(\frac{\mu_b\mu_0}{\varepsilon_b\epsilon_0}\right)^{1/2}, \quad (8)$$

where $\mathbf{S}_{\mathrm{i}}(\mathbf{0})$ is the time-averaged incident Poynting vector, $\mathbf{S}_{\mathrm{i}}(\mathbf{r})\equiv\frac{1}{2}\mathrm{Re}\{\mathbf{E}_{\mathrm{i}}^{*}\times\mathbf{H}_{\mathrm{i}}\}$, evaluated at the origin.

For an incident homogeneous plane-polarized wave, the normalization of Eq. (8) is consistent with A being the amplitude of a complex electric field, $|\mathbf{E}_{\mathrm{i}}^{\mathrm{p.w.}}|=A$. The adoption of Eq. (8) imposes a normalization condition on the dimensionless a coefficients. A computation of $|\mathbf{S}_{\mathrm{i}}(\mathbf{0})|$ using the field developments of Eqs. (4) and (6) and the value Eq. (8) of A shows that the dimensionless incident-field coefficient vector a must consequently be normalized such that the dipole beam coefficients satisfy (see Appendix D)

$$\mathrm{Re}\{[a]_{1,-1}^{\mathrm{N},*}[a]_{1,-1}^{\mathrm{M}} - [a]_{1,1}^{\mathrm{N},*}[a]_{1,1}^{\mathrm{M}}\} = 6\pi. \quad (9)$$

One can verify that the plane-wave coefficients of Eqs. (7) [see also Eqs. (15) below] always satisfy this normalization condition.

The direction of incidence, $\hat{\mathbf{u}}_{\mathrm{i}}$, of the incident field is defined as

$$\hat{\mathbf{u}}_{\mathrm{i}} \equiv \mathbf{S}_{\mathrm{i}}(\mathbf{0})/|\mathbf{S}_{\mathrm{i}}(\mathbf{0})|, \quad (10)$$

with $\hat{\mathbf{u}}_{\mathrm{i}}$ characterized by two angles, θ_{i} and ϕ_{i}. For axisymmetric beams, $\hat{\mathbf{u}}_{\mathrm{i}}$ will lie along the symmetry axis. We henceforth define the incident irradiance, $I(\mathbf{r})$, of the incident field as the beam power flux along the direction of incidence:

$$I(\mathbf{r}) \equiv \mathbf{S}_{\mathrm{i}}(\mathbf{r})\cdot\hat{\mathbf{u}}_{\mathrm{i}}, \quad (11)$$

where it is important to note that $I(\mathbf{r})$ for inhomogeneous beams is not equal to the norm of the Poynting vector, $|\mathbf{S}_{\mathrm{i}}(\mathbf{r})|$ (except at the origin).

The total beam power, P_{i}, is a more readily obtainable experimental quantity than $I(\mathbf{0})$. Furthermore, for more exotic beams (doughnut beams, asymmetric beams, etc.), the maximal symmetry point may not always be readily identifiable or may be located in a region of near-zero irradiance. We will see in Section 3 below how one can reformulate the force in terms of a beam power normalization that is independent of a chosen point of system origin. For the moment, we remark that P_{i} can be obtained by integrating the irradiance over any plane perpendicular to $\hat{\mathbf{u}}_{\mathrm{i}}$; i.e., when $\hat{\mathbf{z}}\equiv\hat{\mathbf{u}}_{\mathrm{i}}$, P_{i} is given by

$$P_{\mathrm{i}} = \int I(x,y,z)\mathrm{d}x\mathrm{d}y|_{z=\mathrm{const.}} = \int_0^{\infty}\rho\mathrm{d}\rho\int_0^{2\pi}\mathrm{d}\phi I(\rho,\phi,z)|_{z=\mathrm{const.}}, \quad (12)$$

independent of z.

B. Axisymmetric Beams

In this paper, we will consider only beams whose irradiance is axisymmetric. We shall see below, however, that this does not, in general, imply an axial symmetric intensity, $|\mathbf{E}|^2$. It suffices for this demonstration to perform calculations for models based on low-order Davis corrections[14,15] to moderately divergent beams.

If one develops the partial-wave expansion of a beam with an axisymmetric irradiance in a system whose origin is placed at the center of the maximum beam constriction, the partial-wave expansion coefficients can be conveniently expressed[15] as

$$[a]_{n,m}^{\mathrm{A}} = [g]_n[p]_{n,m}^{\mathrm{A}}, \quad \mathrm{A}=\mathrm{M,N}, \quad (13)$$

where the $[p]_{n,m}^{\mathrm{A}}$ are the plane-wave expansion coefficients of a plane wave with $\hat{\mathbf{k}}=\hat{\mathbf{u}}_{\mathrm{i}}$ and the $[g]_n$ coefficients depend only on the n number. Following the terminology of Gouesebet *et al.*, we refer to these $[g]_n$ coefficients as the beam shape coefficients.

Strictly speaking, the models that we shall consider lie somewhat outside the paraxial approximation invoked in the derivation of a Gaussian beam. Nevertheless, the low-order Davis corrections that we have chosen to work with allow us to roughly apply Gaussian beam terminology such as diffraction length, waist, etc. For near-Gaussian beams, the tightness of the beam focusing can be parameterized via the dimensionless beam shape parameter s:

$$s \equiv \frac{1}{kw_0} \equiv \frac{w_0}{2z_R} \simeq \frac{\tan\theta_d}{2}, \tag{14}$$

where w_0 in the paraxial approximation is the minimal beam radius or waist, z_R is the Rayleigh diffraction length, and θ_d is the beam angle of divergence. The first equality in expression (14) gives us a physically transparent expression of the s parameter as the wavelength divided by beam circumference at the minimal focus (i.e., the circumference of the beam spot).

Using the values of the plane-wave coefficients given in Eqs. (7) and defining the $\hat{\mathbf{z}}$ axis to lie along the incident-beam direction, we find that the analytic expressions of the $|m|=1$ plane-wave coefficients are

$$[p]^{\mathrm{M}}_{n,1} \equiv 4\pi\mathcal{X}_{n1}(0,0)\cdot\hat{\mathbf{e}}_{\mathrm{i}} = i^n\sqrt{\pi(2n+1)}(i\hat{\theta}+\hat{\phi})\cdot\hat{\mathbf{e}}_{\mathrm{i}},$$

$$[p]^{\mathrm{N}}_{n,1} \equiv 4\pi\mathcal{Z}_{n1}(0,0)\cdot\hat{\mathbf{e}}_{\mathrm{i}} = i^n\sqrt{\pi(2n+1)}(i\hat{\theta}+\hat{\phi})\cdot\hat{\mathbf{e}}_{\mathrm{i}},$$

$$[p]^{\mathrm{M}}_{n,-1} = i^n\sqrt{\pi(2n+1)}(i\hat{\theta}-\hat{\phi})\cdot\hat{\mathbf{e}}_{\mathrm{i}},$$

$$[p]^{\mathrm{N}}_{n,-1} = i^n\sqrt{\pi(2n+1)}(-i\hat{\theta}+\hat{\phi})\cdot\hat{\mathbf{e}}_{\mathrm{i}}, \tag{15}$$

with $[p]^{\mathrm{M,N}}_{n,m}=0$, when $|m|\neq 1$. Under our chosen conditions that the origin is the maximum symmetry point of the beam, the beam shape coefficients can be chosen to be real.[15] One further ensures that the beam expansion coefficients, $[a]^{\mathrm{A}}_{n,m}$ [Eq. (13)], satisfy the normalization condition of Eq. (9) by simply imposing $[g]_1=1$ [in that the plane-wave coefficients, $[p]^{\mathrm{A}}_{1,m}$, already satisfy Eq. (9)].

C. Beam Power Normalization

We saw in Eq. (8) that the beam amplitude constant, A, was determined by the irradiance at the origin $I(\mathbf{0})$. This beam center irradiance is rarely a precisely known quantity, and the relationship between $I(\mathbf{0})$ and the total beam power depends strongly on the beam shape. It is therefore preferable to formulate the force in terms of the total beam power P_{i}. Dimensional arguments lead us to a convenient definition of a dimensionless shape normalization parameter, φ, defined such that

$$I(\mathbf{0}) \equiv \varphi\frac{k^2P_{\mathrm{i}}}{\pi}, \tag{16}$$

where $k=2\pi/\lambda_b$, the factor π is for later convenience, and φ is a geometric factor calculated from the irradiance profile of the beam. For an axisymmetric beam, the total power is

$$P_{\mathrm{i}} = \left.\frac{2\pi}{k^2}\int_0^\infty I(\mathbf{r})k\rho(k\,\mathrm{d}\rho)\right|_{z=\mathrm{const.}}. \tag{17}$$

A comparison with Eq. (16) shows that φ is expressed as

$$\varphi = \left[2\int_0^\infty \frac{I(\mathbf{r})}{I(\mathbf{0})}k\rho(k\,\mathrm{d}\rho)\right|_{z=\mathrm{const.}}\Bigg]^{-1}. \tag{18}$$

The extent to which an optical tweezer beam differs from a paraxial Gaussian beam approximation is an important question in optical tweezers, and it may therefore prove instructive for comparison to calculate φ for a Gaussian beam. We recall that Gaussian beams are an approximate solution of the Maxwell equations in free space for which the irradiance is expressed as

$$I_g(\mathbf{r}) = I_g(\mathbf{0})\left[\frac{w_0}{w(z)}\right]^2\exp\left[-\frac{2\rho^2}{w^2(z)}\right];$$

$$w(z) = w_0\left[1+\left(\frac{z}{z_R}\right)^2\right]^{1/2}, \tag{19}$$

where $z_R=kw_0^2/2=w_0/2s$ is the Rayleigh length and s is the beam parameter of expression (14). The power integral of Eq. (17) for a Gaussian irradiance yields

$$P^g_{\mathrm{i}} = \frac{\pi}{2}w_0^2I_g(\mathbf{0}) = \frac{\pi}{2}\frac{1}{k^2s^2}I_g(\mathbf{0}),$$

which corresponds to a normalization factor from Eq. (18) of $\varphi_g=2s^2$.

For non-Gaussian beams, one can readily evaluate φ numerically by carrying out the integral of Eq. (18) in an arbitrary $z=$constant plane. With a bit of effort, one can alternatively obtain an analytic expression for φ in terms of the shape coefficients. One possible derivation of this analytic expression is outlined in Appendix C by our carrying out an analytic integration of the irradiance in the $z=0$ plane. The result in terms of the shape coefficients, $[g]_n$, of Eq. (13) is

$$\varphi = \left\{\sum_{p,q=0}^{(N_{\max}-1)/2}[g]_{2p+1}[g]_{2q+1}(4p+3)(4q+3)\times\frac{(2p-1)!!}{(2p+2)!!}\frac{(2q-1)!!}{(2q+2)!!}(-1)^{p-q} + 2\sum_{p=1}^{N_{\max}/2}\sum_{q=0}^{(N_{\max}-1)/2}[g]_{2p}[g]_{2q+1}\frac{(2q+1)!!}{(2q)!!}\times\frac{(2p-1)!!}{(2p)!!}\frac{(4p+1)(4q+3)}{2p(2p+1)-(2q+1)(2q+2)}(-1)^{p-q+1}\right\}^{-1}. \tag{20}$$

We note that a statement has erroneously appeared in the literature that the power of inhomogeneous beams is simply $P_{\mathrm{i}}\propto\Sigma_{n,m}\{|a^{\mathrm{M}}_{n,m}|^2+|a^{\mathrm{N}}_{n,m}|^2\}$. This result is apparently derived through far-field considerations of the intensity and an overly hasty appeal to the orthonormality of the VSHs. It is worth remarking that the erroneous result predicts that the total power flux of an inhomogeneous beam is simply the sum of the power flux of the individual partial waves (without interference effects). If any further evidence were necessary, we remark that it is a relatively simple matter to numerically compute the beam irradiance over any infinite plane intercepting the beam and that this calculation supports Eq. (20).

D. Davis-Type Beams

We have chosen to work with Davis-type models here because they allow us to use familiar Gaussian beam terminology and because, in the localization approximation of

Gouesebet *et al.*,[15] one obtains simple analytic expressions for their beam coefficients. Nonparaxial corrections in the Davis prescription take the form of an s^2 power series of approximations to the vector potential, and the first-, third-, and fifth-order Davis beams are given, respectively, by[15]

$$[g_1]_n = \exp[-s^2(n-1)(n+2)],$$

$$[g_3]_n = [g_1]_n + \exp[-s^2(n-1)(n+2)](n-1)(n+2)s^4[3-(n-1)(2+n)s^2],$$

$$[g_5]_n = [g_3]_n + \exp[-s^2(n-1)(n+2)]\{(n-1)^2(n+2)^2s^8[10-5(n-1)(2+n)s^2+0.5(n-1)^2(n+2)^2s^4]\}, \quad (21)$$

where g_1 corresponds to the commonly used paraxial, i.e., Gaussian approximation to focused beams with axial, i.e., E_z, field corrections.[14]

The diffraction limit of focusing is generally accepted to be $w_0 \simeq \lambda_b/2$, which corresponds to an s parameter of $s \equiv \lambda_b/2\pi w_0 \simeq 1/\pi \simeq 0.32$, which we shall adopt from here on. This does not mean that $s \simeq 1/\pi$ is the largest possible beam shape parameter but rather that higher s parameters would require corrections beyond that of the low-order Davis corrections in order to reconcile high beam divergence with diffraction considerations. Taking $s=1/\pi$ (corresponding to a beam divergence of $\theta_d \simeq 33°$), we illustrate the focal-plane irradiance and intensity profiles for a g_5 beam in Fig. 1. The shape normalization factor for this beam is $\varphi_{g_5} \simeq 0.130$ (as opposed to a Gaussian value of $\varphi = 2s^2 \simeq 0.2$; we note that the considerable difference between these two values of φ is due in part to the non-Gaussian nature of the g_5 beam and in part to ambiguities involving the determination of w_0 in terms of irradiance or intensity).

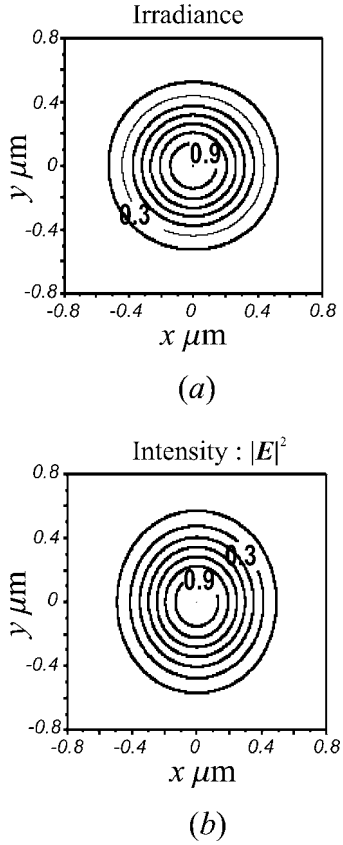

Fig. 1. Focal-plane irradiance and intensity of a $\hat{\mathbf{y}}$-polarized fifth-order Davis beam with $s=1/\pi$.

3. CROSS SECTIONS AND OPTICAL FORCES IN INHOMOGENEOUS BEAMS

For inhomogeneous beams, it proves essential to define position-dependent cross sections and efficiencies. We introduce our notation and justify our terminology by first studying the position-dependent scattering cross section in inhomogeneous beams. We then tackle the somewhat more difficult problem of optical force cross sections and efficiencies.

A. Position-Dependent Cross Sections

Before generalizing to inhomogeneous beams, let us first recall the traditional definition of the scattering cross section. For incident plane waves, the total electromagnetic power scattered by a particle is given by $P_s = I\sigma_s$, where the scattering cross section, σ_s, has the dimension of a surface. The irradiance is defined by $I \equiv \mathbf{S}_i \cdot \hat{\mathbf{k}}_i = |\mathbf{S}_i|$, where $\mathbf{S}_i$ is the complex Poynting vector of the chosen incident plane wave. The σ_s depends on the physical properties of the particle, as well as the wavelength, direction, and polarization of the incident field, but not on the particle position or incident-field strength. By definition, σ_s is the solid-angle integral of the differential cross section, $d\sigma_s/d\Omega$:

$$\sigma_s(\theta_i, \phi_i) = \int_0^{\pi} \sin\theta \mathrm{d}\theta \int_0^{2\pi} \mathrm{d}\phi \frac{\mathrm{d}\sigma_s(\theta, \phi, \theta_i, \phi_i)}{\mathrm{d}\Omega}, \quad (22)$$

where θ_i, ϕ_i specify the direction of $\hat{\mathbf{k}}_i$. The differential cross section, $\mathrm{d}\sigma_s/\mathrm{d}\Omega$, is defined via the ratio of scattered to incident flux:

$$\frac{\mathrm{d}\sigma_s(\theta, \phi, \theta_i, \phi_i)}{\mathrm{d}\Omega} \equiv \lim_{r\to\infty} r^2 \frac{\hat{\mathbf{r}} \cdot \mathbf{S}_s(\mathbf{r})}{I}, \quad (23)$$

where $\mathbf{S}_s(r\hat{\mathbf{r}})$ is the Poynting vector of the scattered field and the angles θ, ϕ specify the direction of $\hat{\mathbf{r}}$.

For inhomogeneous beams, the irradiance [see Eqs. (10) and (11)] is no longer a constant, and the scattered flux will depend on the particles' position. For a particle centered on $\mathbf{x}$, we can generalize the cross-section formula of Eq. (23) by dividing by the irradiance at the system origin, $I(\mathbf{0}) \equiv \mathbf{S}_i(\mathbf{0}) \cdot \hat{\mathbf{u}}_i = |\mathbf{S}_i(\mathbf{0})|$:

$$\frac{\mathrm{d}\sigma_s(\mathbf{x})}{\mathrm{d}\Omega} \equiv \lim_{r\to\infty} r^2 \frac{\hat{\mathbf{r}} \cdot \mathbf{S}_s(\mathbf{r})}{I(\mathbf{0})} = \lim_{r\to\infty} \frac{r^2}{2} \left(\frac{\varepsilon_b \epsilon_0}{\mu_b \mu_0}\right)^{1/2} \frac{\mathbf{E}_s^*(\mathbf{r}) \cdot \mathbf{E}_s(\mathbf{r})}{I(\mathbf{0})}. \quad (24)$$

The power of the radiation scattered by a particle at position $\mathbf{x}$ is then $P_s(\mathbf{x}) = I(\mathbf{0})\sigma_s(\mathbf{x})$.

The position dependence in Eq. (24) enters into the calculations via the VSWF development of the scattered field:

$$\mathbf{E}_s(\mathbf{r}') = A\mathcal{R}g\{\mathbf{\Psi}^t[k(\mathbf{r}-\mathbf{x})]\}f(\mathbf{x}), \tag{25}$$

where $\mathbf{r}' \equiv \mathbf{r}-\mathbf{x}$ and $f(\mathbf{x})$ is the column vector composed of the scattering coefficients for a particle centered on $\mathbf{x}$. One obtains an analytic expression for $\sigma_s(\mathbf{x})$ in terms of $f(\mathbf{x})$ by inserting the partial-wave development of Eq. (25) into Eq. (24), invoking Eq. (8) for the value of A, and carrying out an analytic integration over the solid angles in Eq. (22) to obtain[11,16]

$$\sigma_s(\mathbf{x}) = \frac{1}{k^2} f^\dagger(\mathbf{x}) f(\mathbf{x}). \tag{26}$$

For incident-field coefficients, $a(\mathbf{x})$, developed around an origin located at $\mathbf{x}$ in the system reference frame, the scattering coefficients can be conveniently obtained from transition-matrix theory as

$$f(\mathbf{x}) = Ta(\mathbf{x}), \tag{27}$$

where T is the transition matrix of the scattering particle.[11,16] The translation-addition theorem (see Appendix B) allows us to express $a(\mathbf{x})$ in terms of the incident-field coefficients, a, established in the system reference frame:

$$a(\mathbf{x}) = J(k\mathbf{x})a, \tag{28}$$

where $J(k\mathbf{x})$ is the regular translation-addition matrix. This leaves us with a final expression for the position-dependent cross section:

$$\sigma_s(\mathbf{x}) = \frac{1}{k^2} a^\dagger J^\dagger(k\mathbf{x}) T^\dagger T J(k\mathbf{x}) a. \tag{29}$$

This expression for $\sigma_s(\mathbf{x})$ has two inconvenient aspects: The value of $\sigma_s(\mathbf{x})$ will depend on the choice of the system origin, and the formula in Eq. (29) is valid only if the system incident-field coefficients, a, satisfy the normalization of Eq. (9). Both problems can be removed by one's formulating the scattering power in terms of the total incident-beam power. Invoking the shape normalization parameter, φ, of Eq. (16), we can write the expression for the scattered power, $P_s(\mathbf{x}) = I(\mathbf{0})\sigma_s(\mathbf{x})$, in terms of the total power, P_i, of the incident beam:

$$P_s(\mathbf{x}) = P_i \frac{k^2}{\pi} \varphi \sigma_s(\mathbf{x}) \equiv P_i Q_s(\mathbf{x}),$$

$$Q_s(\mathbf{x}) \equiv k^2 \frac{\varphi}{\pi} \sigma_s(\mathbf{x}) = \frac{\varphi}{\pi} a^\dagger J^\dagger(k\mathbf{x}) T^\dagger T J(k\mathbf{x}) a, \tag{30}$$

where the dimensionless beam efficiency factor, $Q_s(\mathbf{x})$, is independent of the normalization of the incident-field coefficients, a. Furthermore, $Q_s(\mathbf{x})$ is independent of the choice of system origin.

Having familiarized ourselves with position-dependent cross sections, we will apply analogous considerations and formulations to the force cross sections and efficiencies in Subsection 3.B.

B. Force Cross Formulation from the Maxwell Stress Tensor

Starting from the Lorentz force equations, one can calculate the time-averaged electromagnetic force, $\mathbf{F}$, on the induced charges in a material object by integrating the time-harmonic Maxwell stress tensor, $\vec{\vec{\mathbf{T}}}$, over a closed surface, Γ, surrounding the object:

$$\mathbf{F} = \oint_\Gamma \vec{\vec{\mathbf{T}}} \cdot \hat{\mathbf{n}} ds, \tag{31}$$

where $\hat{\mathbf{n}}$ is the local unit normal of the closed surface. The time-averaged optical force is then obtained by our evaluating the following time-averaged constraint tensor $\vec{\vec{\mathbf{T}}}$ expressed in terms of the total complex electromagnetic fields, $\mathbf{E}$ and $\mathbf{B}$:

$$\vec{\vec{\mathbf{T}}}_{i,j}(\mathbf{r}) = \frac{1}{2}\mathrm{Re}\left\{ \varepsilon_b \epsilon_0 E_i^*(\mathbf{r}) E_j(\mathbf{r}) + \frac{1}{\mu_b \mu_0} B_i^*(\mathbf{r}) B_j(\mathbf{r}) - \frac{1}{2}\left[\varepsilon_b \epsilon_0 |\mathbf{E}(\mathbf{r})|^2 + \frac{|\mathbf{B}(\mathbf{r})|^2}{\mu_b \mu_0} \right] \delta_{i,j} \right\}. \tag{32}$$

One can readily verify that $\vec{\vec{\mathbf{T}}}$ has the dimension of pressure.

To remove the dependence on the field strength, it is convenient to define a vector radiation force cross section $\boldsymbol{\sigma}_f$ and efficiency vector $\mathbf{Q}_f$ such that

$$\mathbf{F} \equiv \frac{I(\mathbf{0})}{v_b} \boldsymbol{\sigma}_f(\mathbf{r}) = \frac{P_i}{v_b} \frac{k^2 \varphi}{\pi} \boldsymbol{\sigma}_f(\mathbf{r}) \equiv \frac{P_i}{v_b} \mathbf{Q}_f(\mathbf{r}), \tag{33}$$

where $v_b = c/n_b = \sqrt{\varepsilon_b \mu_b \epsilon_0 \mu_0}^{-1}$ is the (real) phase velocity in the background medium. With these definitions, the vector $\boldsymbol{\sigma}_f(\mathbf{r})$ has the dimensions of a surface, and $\mathbf{Q}_f(\mathbf{r}) \equiv (k^2\varphi/\pi)\boldsymbol{\sigma}_f(\mathbf{r})$ is an efficiency vector that is independent of the normalization of the incident coefficient vector a.

Taking the closed surface in Eq. (31) to be a sphere at infinity, invoking the far-field limits, and comparing the result with the definitions in Eq. (33) show that $\boldsymbol{\sigma}_f$ can be expressed as

$$\boldsymbol{\sigma}_f = \boldsymbol{\sigma}_r - \boldsymbol{\sigma}_a, \tag{34}$$

where $\boldsymbol{\sigma}_a$ characterizes the contribution to the force due to asymmetric scattering of the particle:

$$\boldsymbol{\sigma}_a = \frac{v_b}{4I(\mathbf{0})} \int_\Omega \hat{\mathbf{r}} \left\{ \varepsilon_b \epsilon_0 \mathbf{E}_s^* \cdot \mathbf{E}_s + \frac{1}{\mu_b \mu_0} \mathbf{B}_s^* \cdot \mathbf{B}_s \right\} d\Omega \underset{r\to\infty}{=} \frac{1}{2I(\mathbf{0})} r^2 \left(\frac{\varepsilon_b \epsilon_0}{\mu_b \mu_0} \right)^{1/2} \int_\Omega \hat{\mathbf{r}} \mathbf{E}_s^* \cdot \mathbf{E}_s d\Omega. \tag{35}$$

We have eliminated the magnetic field from the expressions by using the vector identity $(\mathbf{a}\times\mathbf{b})\cdot(\mathbf{c}\times\mathbf{d}) = (\mathbf{a}\cdot\mathbf{c})\times(\mathbf{b}\cdot\mathbf{d}) - (\mathbf{a}\cdot\mathbf{d})(\mathbf{b}\cdot\mathbf{c})$, the far-field results $\lim_{r\to\infty} \hat{\mathbf{r}}\cdot\mathbf{E}_s = 0$, and[13]

$$\mathbf{B}_s(\mathbf{r}) \underset{r\to\infty}{=} (\varepsilon_b \epsilon_0 \mu_b \mu_0)^{1/2} \hat{\mathbf{r}} \times \mathbf{E}_s. \tag{36}$$

The other contribution to the optical force, $\boldsymbol{\sigma}_r$, corresponds to the momentum flux removed from the incident beam:

$$\begin{aligned}\boldsymbol{\sigma}_r \underset{r\to\infty}{=} & -\frac{v_b}{4I(\mathbf{0})}r^2\left\{\varepsilon_b\epsilon_0\int_\Omega \hat{\mathbf{r}}\,\mathrm{Re}\{\mathbf{E}_s^*\cdot\mathbf{E}_i+\mathbf{E}_i^*\cdot\mathbf{E}_s\}\mathrm{d}\Omega\right.\\ &\left.+\frac{1}{\mu_b\mu_0}\int_\Omega \hat{\mathbf{r}}\,\mathrm{Re}\{\mathbf{B}_s^*\cdot\mathbf{B}_i+\mathbf{B}_i^*\cdot\mathbf{B}_s\}\mathrm{d}\Omega\right\}\\ =&-\frac{1}{2I(\mathbf{0})}\lim_{r\to\infty} r^2\left(\frac{\varepsilon_b\epsilon_0}{\mu_b\mu_0}\right)^{1/2}\int_\Omega \hat{\mathbf{r}}\,\mathrm{Re}\{\mathbf{E}_s^*\cdot\mathbf{E}_i+\mathbf{E}_i^*\cdot\mathbf{E}_s\}\mathrm{d}\Omega,\end{aligned} \tag{37}$$

where we have again eliminated the magnetic field by employing the same techniques outlined after Eq. (35) and using $\lim_{r\to\infty}\mathbf{B}_i(\mathbf{r})=(\varepsilon_b\epsilon_0\mu_b\mu_0)^{1/2}\hat{\mathbf{r}}\times\mathbf{E}_i$.

C. Axial Force Efficiency

In single-beam optical tweezers, trapping is consistently stronger along the radial direction than in the axial direction. To determine the existence of trapping, one must foremost look at the forces along the beam direction (henceforth referred to as the axial direction), which typically go under the name of optical pressure even though trapping can exist only when this quantity has a region of negative values.

Without loss of generality, we can define the $\hat{\mathbf{z}}$ axis to lie along the $\hat{\mathbf{z}}=\hat{\mathbf{u}}_i$ direction. The optical pressure force is thus $F_p=F_z=(P_i/v_b)(k^2\varphi/\pi)\sigma_p$ with

$$\sigma_p\equiv\hat{\mathbf{z}}\cdot\boldsymbol{\sigma}_r-\hat{\mathbf{z}}\cdot\boldsymbol{\sigma}_a\equiv\sigma_r-g\sigma_s, \tag{38}$$

where σ_s is the scattering cross section of Eq. (29) and the asymmetry parameter, g, has a standard definition as the projection of the scattered radiation along the direction of incidence.[13] We obtain an analytic expression for g in terms of the scattering coefficient vector $f(\mathbf{x})$ by inserting the development of $\mathbf{E}_s$ on the VSWF basis, Eq. (25), and carrying out the angular integrations in the $\hat{\mathbf{z}}$ component of Eq. (35). The result is

$$\begin{aligned}g\equiv&\frac{1}{\sigma_s}\hat{\mathbf{z}}\cdot\boldsymbol{\sigma}_a=\frac{1}{2I(\mathbf{0})\sigma_s}\left(\frac{\varepsilon_b\epsilon_0}{\mu_b\mu_0}\right)^{1/2}\lim_{r\to\infty} r^2\int_\Omega \hat{\mathbf{z}}\cdot\hat{\mathbf{r}}\mathbf{E}_s^*\cdot\mathbf{E}_s\mathrm{d}\Omega\\ =&\frac{1}{k^2\sigma_s}f^\dagger(\mathbf{x})\\ &\times\left\{\int \mathrm{d}\Omega\cos\theta\begin{bmatrix}\mathcal{X}(\theta,\phi)\\ \mathcal{Z}(\theta,\phi)\end{bmatrix}\cdot[\mathcal{X}^*(\theta,\phi),\mathcal{Z}^*(\theta,\phi)]\right\}f(\mathbf{x})\\ =&\frac{1}{\sigma_s k^2}f^\dagger(\mathbf{x})\Upsilon f(\mathbf{x}),\end{aligned} \tag{39}$$

where the Υ matrix is obtained by one's carrying out the solid-angle integration of the term in brackets and takes the form

$$\Upsilon=\begin{bmatrix}\Xi & \Theta\\ \Theta & \Xi\end{bmatrix}, \tag{40}$$

$$\Theta_{nm,\nu\mu}=\frac{m}{n(n+1)}\delta_{m,\mu}\delta_{n,\nu},$$

$$\begin{aligned}\Xi_{nm,\nu\mu}=\delta_{m,\mu}\frac{i}{\sqrt{(2n+1)(2\nu+1)}}&\left[\frac{\delta_{\nu,n-1}}{n}\sqrt{(n^2-1)(n^2-m^2)}\right.\\ &\left.-\frac{\delta_{\nu,n+1}}{\nu}\sqrt{(\nu^2-1)(\nu^2-m^2)}\right].\end{aligned} \tag{41}$$

Carrying out similar manipulations for σ_r, we find

$$\begin{aligned}\sigma_r(\mathbf{x})\equiv\hat{\mathbf{z}}\cdot\boldsymbol{\sigma}_r=&-\frac{1}{2I(\mathbf{0})}\left(\frac{\varepsilon_b\epsilon_0}{\mu_b\mu_0}\right)^{1/2}\lim_{r\to\infty} r^2\int_\Omega \hat{\mathbf{z}}\cdot\hat{\mathbf{r}}\,\mathrm{Re}\{\mathbf{E}_s^*\cdot\mathbf{E}_i\\ &+\mathbf{E}_i^*\cdot\mathbf{E}_s\}\mathrm{d}\Omega=-\frac{1}{k^2}\mathrm{Re}\{a^\dagger(\mathbf{x})\Upsilon f(\mathbf{x})\}.\end{aligned} \tag{42}$$

Recalling the defining property of the transition matrix, Eq. (27), and invoking the regular translation-addition matrix, $J(k\mathbf{x})$ [see Eqs. (28) and (B2)], we find that $\sigma_p=\sigma_r-g\sigma_s$, and the corresponding efficiency vector, $Q_p(\mathbf{x})$, may be conveniently expressed as

$$\begin{aligned}\sigma_p(\mathbf{x})=&-\frac{1}{k^2}\mathrm{Re}\{a^\dagger J^\dagger(k\mathbf{x})\Upsilon T J(k\mathbf{x})a\}\\ &-\frac{1}{k^2}a^\dagger J^\dagger(k\mathbf{x})T^\dagger\Upsilon T J(k\mathbf{x})a,\\ Q_p(\mathbf{x})=&-\frac{\varphi}{\pi}\mathrm{Re}\{a^\dagger J^\dagger(k\mathbf{x})\Upsilon T J(k\mathbf{x})a\}\\ &-\frac{\varphi}{\pi}a^\dagger J^\dagger(k\mathbf{x})T^\dagger\Upsilon T J(k\mathbf{x})a,\end{aligned} \tag{43}$$

where we recall that in terms of $Q_p(\mathbf{x})$ the optical pressure force is simply

$$F_p=\frac{P_i}{v_b}Q_p(\mathbf{x}). \tag{44}$$

The absolute value of the efficiency vector $Q_p(\mathbf{x})$ thus determines the fraction of the total beam momentum that is converted into a force along the direction of incidence. For numerical determinations of the force, the factor $1/v_b$ in Eq. (44) can be approximately expressed as

$$\frac{1}{v_b}\simeq\frac{n_b}{3}10^{-8}\frac{N}{W}=n_b\frac{10}{3}\frac{\mathrm{pN}}{\mathrm{mW}}\simeq 4.4\frac{\mathrm{pN}}{\mathrm{mW}}, \tag{45}$$

where, in the last equality, we took our value for the refraction index of water, $n_b\simeq 1.32$. One can therefore obtain the force in piconewtons per milliwatt of beam power by multiplying $Q_p(\mathbf{x})$ by 4.4.

We remark that, although our force formulas are valid for inhomogeneous beams, one retrieves for incident plane waves the classic Debye–Mie results, $\sigma_p=\sigma_e-g\sigma_s$.[13,17,18] This can be verified by showing that the asymmetry factor contribution, $g\sigma_s$ [Eq. (39)], is identical to the plane-wave results[13] by simply inserting the

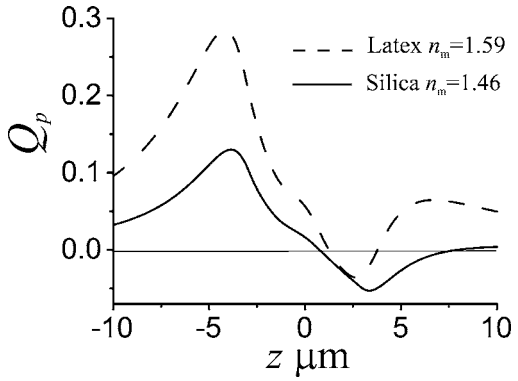

Fig. 2. Axial trapping efficiency, $Q_p(z)$, for spheres of radii $R=2.1$ (μm) composed of silica ($n_s=1.46$) and latex ($n_s=1.59$) immersed in water ($n_b=1.32$) and exposed to a $\hat{\mathbf{y}}$-polarized fifth-order Davis beam.

coefficients for incident plane waves. One can also show that $\sigma_r(\mathbf{x})$ is identical to the extinction cross section σ_e in the plane-wave limit[19]:

$$\sigma_r \to \sigma_e = -\frac{1}{k^2}\mathrm{Re}\{p^\dagger T p\}. \tag{46}$$

D. Applications to Trapping

In this paper we restrict ourselves to evaluating the forces on spherical objects in order to avoid the complications associated with torques and particle orientation. The transition matrix, T, is then diagonal with matrix elements corresponding to the Mie coefficients.[11,16] The axial force formula of expressions (43)–(45) permits us to quantitatively calculate the optical forces along the direction of the beam propagation and thereby determine the trapping position and stiffness.

We show in Fig. 2 the axial trapping efficiency of silica and latex spheres of radius $R=2.1$ (μm) suspended in water and a $\hat{\mathbf{y}}$-polarized, $s=1/\pi$ fifth-order Davis beam. The position $z=0$ corresponds to the beam focus (i.e., center of the Rayleigh region). We note that the calculation predicts trapping for both the silica and the latex spheres because both curves contain regions for which the radiation pressure is negative. The stable trapping position, z_{tr}, is given by the point for which $Q_p(z_{\mathrm{tr}})=0$ and $dQ_p(z)/dz|_{z=z_{\mathrm{tr}}}<0$. We remark that the trapping positions for the two types of sphere, though not the the same, are $\sim$0.8–1 (μm) after the beam focus, which indicates that scattering forces (sometimes called radiation damping forces) along the direction of beam propagation are not entirely negligible compared with the gradient forces that draw the particle toward the beam focus.

Our rigorous calculations permit us to demonstrate the importance of resonance effects on optical forces. Such effects cannot be explored by any of the commonly used approximations such as dipole, geometrical optics, or Born-type approximations. We illustrate in Fig. 3 that resonance effects can have a sizable effect on the axial trapping position of a particle. In Fig. 3, the trapping position is calculated as a function of the sphere radius for silica and latex spheres trapped in water by a fifth-order Davis beam. For radii in which the points on the trapping position curve lie above the $z=R$ dotted line, $R\lesssim 0.62$ (μm) for silica, the center of the beam focus lies outside the particle. For larger particles, $R\gtrsim 0.62$ (μm) for silica, the trapping position lies below the $z=R$ line, indicating that the center of the beam focus lies within the particle as arguments from geometrical optics indicate.

We interpret the oscillations in trapping positions as a function of the radii, observed in Fig. 3, as evidence for geometric resonance effects on the trapping force. This is a subject worthy of more detailed investigations. Notably, one should also investigate the behavior of resonance on the radial trapping force. It may also prove instructive to study the correlation of this phenomenon with the strengths of the scattering cross sections and with field energy densities.

E. Radial Force Efficiency

Let us label $\hat{\rho}$ a radial unit vector (in cylindrical coordinates) between the beam axis and the particle center (characterized by the azimuth angle ϕ). The force along this axis is given by

$$F_\rho \equiv \hat{\rho}\cdot\mathbf{F} = \frac{P_i}{v_b}\hat{\rho}\cdot\mathbf{Q}_f = \frac{P_i}{v_b}\hat{\rho}\cdot(\mathbf{Q}_r - \mathbf{Q}_a). \tag{47}$$

The $\hat{\rho}\cdot\mathbf{Q}_a$ contribution to F_ρ can be expressed as

$$\begin{aligned}\hat{\rho}\cdot\mathbf{Q}_a &= \frac{k^2\varphi}{2\pi I(\mathbf{0})}\left(\frac{\varepsilon_b\epsilon_0}{\mu_b\mu_0}\right)^{1/2}\lim_{r\to\infty} r^2\int_\Omega (\hat{\rho}\cdot\hat{\mathbf{r}})\mathbf{E}_s^*\cdot\mathbf{E}_s d\Omega \\ &= \frac{\varphi}{\pi}f^\dagger(\mathbf{x})\mathrm{D}\left(\phi,\frac{\pi}{2},0\right)\left\{\int d\Omega'\cos\theta'\begin{bmatrix}\mathcal{X}(\theta',\phi')\\ \mathcal{Z}(\theta',\phi')\end{bmatrix}\right. \\ &\quad\left.\cdot[\mathcal{X}^*(\theta',\phi'),\mathcal{Z}^*(\theta',\phi')]\right\}\mathrm{D}^\dagger\left(\phi,\frac{\pi}{2},0\right)f(\mathbf{x}),\end{aligned} \tag{48}$$

where the primed angles are measured with respect to the $\hat{\rho}$ axis as the polar direction and the rotation matrix of the VSHs, $\mathrm{D}(\alpha,\beta,\gamma)$, has the form

$$\mathrm{D}(\alpha,\beta,\gamma) \equiv \begin{bmatrix}\mathcal{D}(\alpha,\beta,\gamma) & 0\\ 0 & \mathcal{D}(\alpha,\beta,\gamma)\end{bmatrix}, \tag{49}$$

where α,β,γ are the Euler angles. The $\mathcal{D}(\alpha,\beta,\gamma)$ matrix elements are described in detail in Ref. 20 and are block diagonal in the orbital (multipole) quantum number, n:

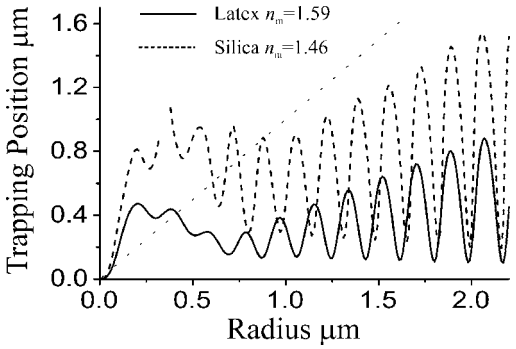

Fig. 3. Trapping positions for silica and latex spheres in water in a $\hat{\mathbf{y}}$-polarized, $s=1/\pi$, fifth-order Davis beam, as a function of the sphere radius.

$$[\mathcal{D}(\alpha,\beta,\gamma)]_{\nu\mu,nm} = \delta_{n,\nu}\exp(i\mu\alpha)d^{(n)}_{\mu m}(\beta)\exp(im\gamma). \quad (50)$$

The elements $d^{(n)}_{\mu m}$ are standard,[20] and expressions for them are given in Appendix B. The integral in brackets in Eq. (48) is the same as that encountered in the axial force, Eq. (39), and, again, yields Υ [see Eq. (40)].

Defining then the matrix

$$\Lambda(\theta,\phi) \equiv \mathrm{D}(\phi,\theta,0)\Upsilon\mathrm{D}^{\dagger}(\phi,\theta,0), \quad (51)$$

and carrying out analogous manipulations on $\hat{\rho}\cdot\mathbf{Q}_{\mathrm{r}}$, we find the final result for Q_ρ is

$$\begin{aligned} Q_\rho \equiv \hat{\rho}\cdot\mathbf{Q}_{\mathrm{f}} = -\frac{\varphi}{\pi}\mathrm{Re}\Bigg[& a^{\dagger}J^{\dagger}(k\mathbf{x})T^{\dagger}\Lambda\left(\frac{\pi}{2},\phi\right)J(k\mathbf{x})a \\ & + a^{\dagger}J^{\dagger}(k\mathbf{x})\Lambda\left(\frac{\pi}{2},\phi\right)TJ(k\mathbf{x})a\Bigg] \\ & - \frac{\varphi}{\pi}a^{\dagger}J^{\dagger}(k\mathbf{x})T^{\dagger}\Lambda\left(\frac{\pi}{2},\phi\right)TJ(k\mathbf{x})a, \end{aligned} \quad (52)$$

where ϕ is the azimuth angle of the particle position $\mathbf{x}$.

In Fig. 4(a), we present the results of calculations of the radial efficiency on a silica sphere with the same particle and beam parameters as in Fig. 2 with a $\hat{\mathbf{y}}$-polarized Davis beam. The particle displacements are restricted to a plane perpendicular to the beam direction $\hat{\mathbf{z}}$ at the axial trapping position determined from Fig. 2, $z_{\mathrm{tr}}\simeq 0.75$ (μm). The radial efficiencies for displacements along the direction of polarization $\hat{\mathbf{y}}$ and perpendicular to it, the $\hat{\mathbf{x}}$ direction, are both displayed.

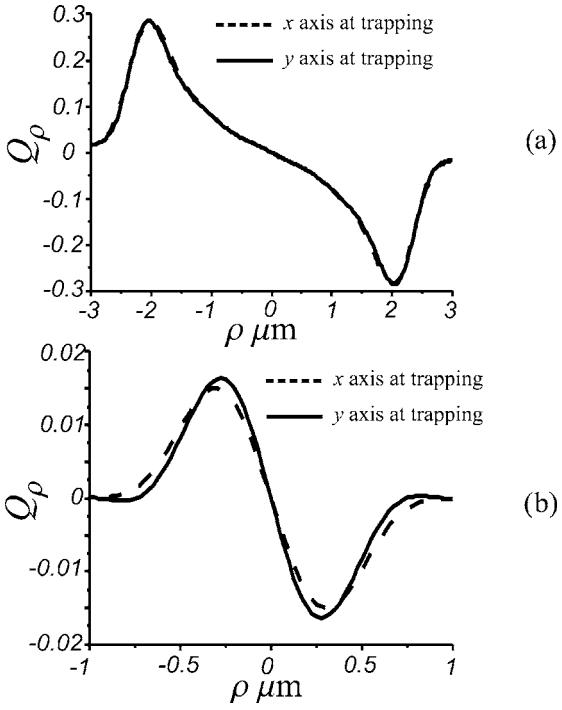

Fig. 4. (a) Radial trapping efficiency, Q_ρ, for a $R=2.1$ (μm) silica as a function of the radial displacements along the $\hat{\mathbf{x}}$ and $\hat{\mathbf{y}}$ axes at the trapping position, $z_{\mathrm{tr}}\simeq 0.75$ (μm). (b) Radial trapping efficiency, Q_ρ, for $\hat{\mathbf{x}}$ and $\hat{\mathbf{y}}$ axis displacements of a $R=0.2$ (μm) silica sphere evaluated at its trapping position $z_{\mathrm{tr}}\simeq 0.43$ (μm).

At least for the beams and particle sizes studied here, the axial asymmetry of the forces is essentially negligible, as can be seen in the example of Fig. 4(a). For smaller particles, the dipole approximation becomes increasingly valid, and it predicts forces more sensitive to the gradient of the axially asymmetric intensity, $|\mathbf{E}_{\mathrm{i}}|^2$, than the (axisymmetric) irradiance, I.[7] We confirm this expectation by calculating in Fig. 4(b) the radial efficiency for a $R=0.2$ (μm) silica sphere at its trapping position, $z_{\mathrm{tr}}\simeq 0.43$ (μm). The axial asymmetry of the optical forces in this situation is considerably more pronounced.

4. CONCLUSIONS

We have hoped to illustrate in this paper that optical forces can be calculated by using rigorous electromagnetic theory in arbitrary directions and for arbitrary particle positions. The formulas that we have developed make use of a unique partial-wave development of the incident beam in an arbitrarily chosen coordinate system, which allows us to choose the system origin such that it facilitates the partial-wave development. Calculations for varying force directions employ the rotation matrices of angular momenta, and the calculation of the force at different particle positions employs the translation-addition theorem. Once one has developed the necessary computer codes, the calculation of the optical forces is generally quite rapid on modern computers and can be used to calculate optical forces in regions that fall outside the domain of validity of commonly invoked approximations. We feel that we have demonstrated the necessity of making such efforts by illustrating the important variations in trapping position that arise owing to geometric resonances within the scattered particles.

APPENDIX A: SPHERICAL WAVES AND VECTOR SPHERICAL HARMONICS

The three normalized VSHs, can be explicitly written in terms of the associated Legendre functions:

$$\mathbf{Y}_{nm}(\theta,\phi) = \gamma_{nm}\sqrt{n(n+1)}P^m_n(\cos\theta)\exp(im\phi)\hat{\mathbf{r}} \equiv Y_{nm}(\theta,\phi)\hat{\mathbf{r}},$$

$$\begin{aligned} \mathbf{X}_{nm}(\theta,\phi) = \gamma_{nm}\Bigg[& \frac{im}{\sin\theta}P^m_n(\cos\theta)\hat{\theta} \\ & - \frac{\mathrm{d}}{\mathrm{d}\theta}P^m_n(\cos\theta)\hat{\phi}\Bigg]\exp(im\phi) \equiv [i\bar{u}^m_n(\cos\theta)\hat{\theta} \\ & - \bar{s}^m_n(\cos\theta)\hat{\phi}]\exp(im\phi), \end{aligned}$$

$$\begin{aligned} \mathbf{Z}_{nm}(\theta,\phi) = \gamma_{nm}\Bigg[& \frac{\mathrm{d}}{\mathrm{d}\theta}P^m_n(\cos\theta)\hat{\theta} \\ & + \frac{im}{\sin\theta}P^m_n(\cos\theta)\hat{\phi}\Bigg]\exp(im\phi) \equiv [\bar{s}^m_n(\cos\theta)\hat{\theta} \\ & + i\bar{u}^m_n(\cos\theta)\hat{\phi}]\exp(im\phi), \end{aligned} \quad (A1)$$

where the normalization coefficients γ_{nm} are defined

$$\gamma_{nm} \equiv \left[\frac{(2n+1)(n-m)!}{4\pi n(n+1)(n+m)!} \right]^{1/2}. \tag{A2}$$

APPENDIX B: ADDITION THEOREM AND ROTATION MATRICES

In optical tweezers containing a single particle, we need only the translation-addition theorem as it applies to regular partial waves. In the context of a given fixed coordinate system and origin, the translation-addition theorem[21,22] takes the form of a translation-addition matrix, $J(k\mathbf{x})$, which permits the development of a partial-wave basis centered on a point $\mathbf{x}$ [i.e., $\mathcal{R}g\{\Psi^t(k\mathbf{r}')\}$, $\mathbf{r}' \equiv \mathbf{r}-\mathbf{x}$] into the regular spherical wave basis centered on the system origin [$\mathcal{R}g\{\Psi(k\mathbf{r})\}$; see Eq. (5)]:

$$\mathcal{R}g\{\Psi(k\mathbf{r})\} = \mathcal{R}g\{\Psi^t(k\mathbf{r}')\}J(k\mathbf{x}), \quad \forall\, |\mathbf{r}_j|, \tag{B1}$$

where J is a matrix of the form

$$J(k\mathbf{x}) \equiv \begin{bmatrix} \bar{A}(k\mathbf{x}) & \bar{B}(k\mathbf{x}) \\ \bar{B}(k\mathbf{x}) & \bar{A}(k\mathbf{x}) \end{bmatrix}. \tag{B2}$$

The matrix elements $\bar{A}_{\nu\mu,nm}$ and $\bar{B}_{\nu\mu,nm}$ are normalized versions of the matrix elements derived by Stein and Cruzan.[11,21,22,23]

The $d^{(n)}_{\mu,m}$ of Eq. (50) can be expressed in terms of the Jacobi polynomials[20]:

$$d^{(n)}_{\mu m}(\beta) = \left[\frac{(n+\mu)!\,(n-\mu)!}{(n+m)!\,(n-m)} \right]^{1/2} \times \left(\cos\frac{\beta}{2} \right)^{m+\mu} \left(\sin\frac{\beta}{2} \right)^{m-\mu} P^{(\mu-m,m+\mu)}_{n-\mu}(\cos\beta). \tag{B3}$$

APPENDIX C: BEAM IRRADIANCE

The power of an incident beam is calculated by one's integrating the normal component of the complex incident Poynting vector, $\mathbf{S}_\mathrm{i}$, over any infinite surface intercepting the beam. As in the text, we find it convenient to adopt for this surface an infinite plane whose unit normal is parallel to the beam direction, $\hat{\mathbf{u}}_\mathrm{i}$. The calculation of beam power then corresponds to an integration of the beam irradiance, $I(\mathbf{r}) \equiv \mathbf{S}_\mathrm{i}\cdot\hat{\mathbf{u}}_\mathrm{i}$, over this plane.

The fact that we use spherical coordinates for the wave functions makes it difficult to perform an analytical integration of $I(\mathbf{r})$ in an arbitrary $z=$constant plane (with $\hat{\mathbf{u}}_\mathrm{i} = \hat{\mathbf{z}}$). It is possible, however, to perform analytic integrations in the $z=0$ plane. With the field VSWF field developments of Eqs. (4) and (6), the irradiance for time-harmonic fields is explicitly

$$\begin{aligned} I(\mathbf{r}) &= \frac{1}{2}\mathrm{Re}\{\mathbf{E}^*_\mathrm{i} \times \mathbf{H}_\mathrm{i}\}\cdot\hat{\mathbf{z}} \\ &= -\frac{1}{2}\left(\frac{\varepsilon_b\epsilon_0}{\mu_b\mu_0}\right)^{1/2} A^2 \sum_{n,m;\nu\mu} \mathrm{Re}\{-i[a^{\mathrm{M},*}_{nm}\mathcal{R}g\{\mathbf{M}^*_{nm}(k\mathbf{r})\} \\ &\quad + a^{\mathrm{N},*}_{nm}\mathcal{R}g\{\mathbf{N}^*_{nm}(k\mathbf{r})\}] \times [a^{\mathrm{M}}_{\nu\mu}\mathcal{R}g\{\mathbf{N}_{\nu\mu}(k\mathbf{r})\} \\ &\quad + a^{\mathrm{N}}_{\nu\mu}\mathcal{R}g\{\mathbf{M}_{\nu\mu}(k\mathbf{r})\}]\cdot\hat{\mathbf{z}}\}. \end{aligned} \tag{C1}$$

The $z=0$ irradiance integral then corresponds to taking $\theta=\pi/2$ and integrating over $\phi=0\to 2\pi$ and $r=0\to\infty$.

An inspection of Eq. (C1) shows that an analytic calculation of the beam power, Eq. (17), will involve four integrals involving vector products of the VSWFs. The contribution to the total beam power involving the coefficient product $a^{\mathrm{M},*}_{nm}a^{\mathrm{N}}_{\nu\mu}$ (denoted δP^{MN}) is zero because $\mathcal{R}g\{\mathbf{M}^*_{nm}\} \times \mathcal{R}g\{\mathbf{M}_{\nu\mu}\}\cdot\hat{\mathbf{z}}=0$ in the $z=0$ plane. The vector product involving $a^{\mathrm{N},*}_{nm}a^{\mathrm{M}}_{\nu\mu}$ (denoted δP^{NM}) does, however, have a nonzero contribution to the power integral of Eq. (17), namely,

$$\begin{aligned} \delta P^{\mathrm{NM}} &= \int_0^\infty r\mathrm{d}r \int_0^{2\pi} \mathrm{d}\phi\, \mathrm{Re}\{-i[a^{\mathrm{N},*}_{nm}a^{\mathrm{M}}_{\nu\mu}\mathcal{R}g\{\mathbf{N}^*_{nm}(k\mathbf{r})\} \\ &\quad \times \mathcal{R}g\{\mathbf{N}_{\nu\mu}(k\mathbf{r})\}]\}\cdot\hat{\mathbf{z}}_{\theta=\pi/2} \\ &= -A^2\frac{\pi}{k^2}\left(\frac{\varepsilon_b\epsilon_0}{\mu_b\mu_0}\right)^{1/2} \sum_{n,\nu,m=\pm1} \mathrm{Re}\{[a]^{\mathrm{N}*}_{nm}[a]^{\mathrm{M}}_{\nu m}\} \\ &\quad \times \frac{\bar{u}^m_n(0)\bar{u}^m_\nu(0)}{m} \times \left\{ n(n+1)\int_0^\infty \frac{j_n(x)}{x}[xj_\nu(x)]'\mathrm{d}x + \nu(\nu \right. \\ &\quad \left. +1)\int_0^\infty [xj_n(x)]'\frac{j_\nu(x)}{x}\mathrm{d}x \right\}, \end{aligned} \tag{C2}$$

where the $\bar{u}^m_n(\cos\theta)$ are defined in Eq. (A1). One finds that $\bar{u}^m_n(0)\bar{u}^m_\nu(0)$ with $|m|=1$ is nonzero only if both n and ν are odd. The analytic expression for $\bar{u}^m_n(0)\bar{u}^m_\nu(0)$ with both n and ν odd is

$$\bar{u}^m_n(0)\bar{u}^m_\nu(0) = \frac{(-1)^{(n-\nu)/2}}{4\pi}\sqrt{(2n+1)(2\nu+1)}\frac{(n-2)!!}{(n+1)!!}\frac{(\nu-2)!!}{(\nu+1)!!}. \tag{C3}$$

The Bessel function integral gives a particularly simple result,

$$n(n+1)\int_0^\infty \frac{j_n(x)}{x}[xj_\nu(x)]'\mathrm{d}x + \nu(\nu+1)\int_0^\infty [xj_n(x)]'\frac{j_\nu(x)}{x}\mathrm{d}x = (-1)^{(n-\nu)/2}, \tag{C4}$$

to yield finally

$$\delta P^{\mathrm{NM}} = -\frac{|I(\mathbf{0})|}{2k^2}\sum_{p,q=0}^{(N_{\max}-1)/2}\sum_{m=\pm 1}\frac{\mathrm{Re}[\,[a]^{\mathrm{N},*}_{2p+1,m}[a]^{\mathrm{M}}_{2q+1,m}\}]}{m} \times\sqrt{(4p+3)(2q+3)}\frac{(2p-1)!!}{(2p+2)!!}\frac{(2q-1)!!}{(2q+2)!!}, \quad \text{(C5)}$$

where $N_{\max}$ is an appropriate cutoff for the VSWF development of the incident beam and $2p+1$ and $2q+1$ are odd integers.

Finally, using the defining property of the beam shape coefficients, g_n, of Eq. (16) and the expressions for the $[p]^{\mathrm{M,N}}_{n,m}$ of Eqs. (15), we can write this sum directly in terms of g_n:

$$\delta P^{\mathrm{NM}} = I(\mathbf{0})\frac{\pi}{k^2}\sum_{p,q=0}^{(N_{\max}-1)/2} g_{2p+1}g_{2q+1}(4p+3) \times(4q+3)\frac{(2p-1)!!}{(2p+2)!!}\frac{(2q-1)!!}{(2q+2)!!}(-1)^{p-q}. \quad \text{(C6)}$$

Evaluating the remaining δP^{MM} and δP^{NN} contributions to the total beam power in a similar manner and appealing to the defining relation, Eq. (13), for the beam shape normalization factor, φ, yield the analytic expression for φ found in Eq. (20).

APPENDIX D: NORMALIZATION CONDITION OF THE INCIDENT-FIELD COEFFICIENTS

From the partial-wave expression for the irradiance, Eq. (C1), one can determine the normalization condition for the incident-field coefficients, Eq. (9), by noting that, as $\mathbf{r}\to\mathbf{0}$, only the $\mathcal{R}g\{\mathbf{N}_{1,m}(k\mathbf{r})\}$ VSWFs are nonzero, and that

$$\begin{aligned}\mathcal{R}g\{\mathbf{N}^{*}_{1m}(k\mathbf{r})\}\times\mathcal{R}g\{\mathbf{N}_{1\mu}(k\mathbf{r})\}\cdot\hat{\mathbf{z}} &= \frac{\sqrt{2}j_1(kr)[krj_1(kr)]'Y^{*}_{1m}(\hat{\mathbf{r}})\mathbf{X}_{1\mu}(\hat{\mathbf{r}})}{k^2r^2} \\ &- \frac{\sqrt{2}[krj_1(kr)]'j_1(kr)Y_{1\mu}(\hat{\mathbf{r}})\mathbf{X}^{*}_{1m}(\hat{\mathbf{r}})}{k^2r^2} \\ &- \frac{[(krj_\nu(kr)]')^2\mathbf{Z}^{*}_{nm}(\theta,\phi)\cdot\mathbf{X}_{\nu\mu}(\theta,\phi)\hat{\mathbf{r}}}{k^2r^2}. \end{aligned} \quad \text{(D1)}$$

Using the limits

$$\lim_{x\to 0} j_1(x)\approx\frac{x}{3}, \quad \lim_{x\to 0}[xj_\nu(x)]'\approx\frac{2x}{3}, \quad \text{(D2)}$$

we obtain

$$\begin{aligned}&\frac{1}{2\pi}\int_0^{2\pi}\mathrm{d}\phi\sum_{m,\mu=-1}^{1}a^{\mathrm{N},*}_{1m}a^{\mathrm{M}}_{1\mu}\mathcal{R}g\{\mathbf{N}^{*}_{1m}(\mathbf{0})\}\times\mathcal{R}g\{\mathbf{N}_{1\mu}(\mathbf{0})\}\cdot\hat{\mathbf{z}}\Big|_{\theta=\pi/2} \\ &= -i\frac{8}{9}\sum_{m=\pm 1}ma^{\mathrm{N},*}_{1,m}a^{\mathrm{M}}_{1,m}\bar{u}^{m}_{1}(0)\bar{u}^{m}_{1}(0) \\ &= \frac{i}{6\pi}\{a^{\mathrm{N},*}_{1,-1}a^{\mathrm{M}}_{1,-1}-a^{\mathrm{N},*}_{1,1}a^{\mathrm{M}}_{1,1}\}, \end{aligned} \quad \text{(D3)}$$

where we used $\bar{u}^{m}_{1}(0)=-\frac{1}{4}\sqrt{3/\pi}$. Putting this result into Eq. (C1), we find that the irradiance at the system origin takes the form

$$\begin{aligned}I(\mathbf{0}) &= \frac{1}{2}\left(\frac{\varepsilon_b\epsilon_0}{\mu_b\mu_0}\right)^{1/2}A^2\frac{1}{6\pi}\mathrm{Re}\{a^{\mathrm{N},*}_{1,-1}a^{\mathrm{M}}_{1,-1}-a^{\mathrm{N},*}_{1,1}a^{\mathrm{M}}_{1,1}\} \\ &= \frac{|\mathbf{S}(\mathbf{0})|}{6\pi}\mathrm{Re}\{a^{\mathrm{N},*}_{1,-1}a^{\mathrm{M}}_{1,-1}-a^{\mathrm{N},*}_{1,1}a^{\mathrm{M}}_{1,1}\}, \end{aligned} \quad \text{(D4)}$$

where we have invoked Eq. (8) for A^2. Because $I(\mathbf{0})=|\mathbf{S}(\mathbf{0})|$, this leads to the normalization condition of Eq. (9) for $a^{\mathrm{M}}_{n,m}$.

As we have seen in the text, the resulting normalization condition, Eq. (9), is trivial to implement, but it is principally only of use when studying and comparing beam profiles. One should keep in mind that the final formulas for the optical forces, Eqs. (43) and (52), are independent of the normalization of the incident-beam coefficients.

The authors thank Gerard Tayeb for numerous helpful discussions and encouragement.

B. Stout, the corresponding author, can be reached by e-mail at brian.stout@fresnel.fr.

REFERENCES

1. A. Ashkin, J. M. Dziedzic, J. E. Bjorkholm, and S. Chu, "Observation of a single-beam gradient force optical trap for dielectric particles," Opt. Lett. **11**, 288–290 (1986).
2. J. C. Crocker, J. A. Matteo, A. D. Dinsmore, and A. G. Yodh, "Entropic attraction and repulsion in binary colloids probed with a line optical tweezer," Phys. Rev. Lett. **82**, 4352–4355 (1999).
3. L. Paterson, M. P MacDonald, J. Arit, W. Dultz, H. Schmitzer, W. Sibett, and K. Dholakia, "Controlled simultaneous rotation of multiple optically trapped particles," J. Mod. Opt. **50**, 1591–1601 (2003).
4. H. Melville, G. F. Milne, G. C. Spalding, W. Sibbett, K. Dholakia, and D. McGloin, "Optical trapping of three-dimensional structures using dynamic holograms," Opt. Express **1**, 3562–3567 (2003).
5. G. Sinclair, J. Leach, P. Jordan, G. Gibson, E. Yao, Z. J. Laczik, M. J. Padgett, and J. Courtial, "Interactive application in holographic optical tweezers of a multiplane Gerchberg–Saxton algorithm for three-dimensional light shaping," Opt. Express **12**, 1665–1670 (2004).
6. J. Leach, G. Sinclair, P. Jordan, J. Courtil, and M. J. Padgett, "3D manipulation of particles into crystal structures using holographic optical tweezers," Opt. Express **12**, 220–226 (2004).
7. A. Ashkin and J. M. Dziedzic, "Optical trapping and manipulation of viruses and bacteria," Science **2335**, 1517–1520 (1987).
8. A. Ashkin, "Forces of a single-beam gradient laser trap on a dielectric sphere in the ray optics regime," Biophys. J. **61**, 569–582 (1992).
9. T. Tlusty, A. Meller, and R. Bar-Ziv, "Optical gradient forces of strongly localized fields," Phys. Rev. Lett. **81**, 1738–1741 (1998).
10. G. Lenormand, S. Hénon, A. Richert, J. Siméon, and F. Gallet, "Direct measurement of the area expansion and shear moduli of the human red blood cell membrane skeleton," Biophys. J. **81**, 43–56 (2001).
11. L. Tsang, J. A. Kong, and R. T. Shin, *Theory of Microwave Remote Sensing* (Wiley, 1985).

12. W. Chew, *Waves and Fields in Inhomogeneous Media*, Series on Electromagnetic Waves (IEEE, 1990).
13. C. F. Bohren and D. R. Huffman, *Absorption and Scattering of Light by Small Particles* (Wiley-Interscience, 1983).
14. L. W. Davis, "Theory of electromagnetic beams," Phys. Rev. A **19**, 1177–1179 (1979).
15. G. Gouesebet, J. A. Lock, and G. Gréhan, "Partial-wave representations of laser beams for use in light-scattering calculations," Appl. Opt. **34**, 2133–2143 (1995).
16. B. Stout, J.-C. Auger, and J. Lafait, "Individual and aggregate scattering matrices and cross-sections: conservation laws and reciprocity," J. Mod. Opt. **48**, 2105–2128 (2001).
17. H. C. Van de Hulst, *Light Scattering by Small Particles* (Dover, 1957).
18. P. Debye, "Der Lichtdruck auf Kugeln von beliebigem Material," Ann. Phys. (Leipzig) **30**, 57–136 (1909).
19. M. I. Mishchenko, "Radiation force caused by scattering, absorption, and emission of light by nonspherical particles," J. Quant. Spectrosc. Radiat. Transf. **70**, 811–816 (2001).
20. A. R. Edmonds, *Angular Momentum in Quantum Mechanics* (Princeton U. Press, 1960).
21. S. Stein, "Addition theorems for spherical wave function," Q. Appl. Math. **19**, 15–24 (1961).
22. O. R. Cruzan, "Translation addition theorems for spherical vector wave functions," Q. Appl. Math. **20**, 33–40 (1962).
23. B. Stout, J. C. Auger, and J. Lafait, "A transfer matrix approach to local field calculations in multiple-scattering problems," J. Mod. Opt. **49**, 2129–2152 (2002).